Open access • Journal Article • DOI:10.1038/NMAT2471

Switchable self-protected attractions in DNA-functionalized colloids.

Mirjam E. Leunissen, Remi Dreyfus, Fook Chiong Cheong, David G. Grier ...+3 more authors

Institutions: New York University

Published on: 14 Jun 2009 - Nature Materials (Nature Publishing Group)

Topics: Sticky and blunt ends

Switchable self-protected attractions in DNA-functionalized colloids

Mirjam Leunissen, Rémi Dreyfus, Fook Cheong, David Grier, Roujie Sha, Nadrian Seeman, Paul Chaikin

LETTERS
PUBLISHED ONLINE: 14 JUNE 2009 | DOI: 10.1038/NMAT2471
nature materials

Switchable self-protected attractions in DNA-functionalized colloids

Mirjam E. Leunissen[1]*, Rémi Dreyfus[1], Fook Chiong Cheong[1], David G. Grier[1], Roujie Sha[2], Nadrian C. Seeman[2] and Paul M. Chaikin[1]

Surface functionalization with DNA is a powerful tool for guiding the self-assembly of nanometre- and micrometre-sized particles[1–11]. Complementary 'sticky ends' form specific inter-particle links and reproducibly bind at low temperature and unbind at high temperature. Surprisingly, the ability of single-stranded DNA to form folded secondary structures has not been explored for controlling (nano) colloidal assembly processes, despite its frequent use in DNA nanotechnology[12–14]. Here, we show how loop and hairpin formation in the DNA coatings of micrometre-sized particles gives us *in situ* control over the inter-particle binding strength and association kinetics. We can finely tune and even switch off the attractions between particles, rendering them inert unless they are heated or held together—like a nano-contact glue. The novel kinetic control offered by the switchable self-protected attractions is explained with a simple quantitative model that emphasizes the competition between intra- and inter-particle hybridization, and the practical utility is demonstrated by the assembly of designer clusters in concentrated suspensions. With self-protection, both the suspension and assembly product are stable, whereas conventional attractive colloids would quickly aggregate. This remarkable functionality makes our self-protected colloids a novel material that greatly extends the utility of DNA-functionalized systems, enabling more versatile, multi-stage assembly approaches.

In many DNA-functionalized systems, the particle association and structural organization are equilibrium processes that depend solely on the system temperature, relative to the particles' DNA-dependent dissociation temperature. This is, for instance, demonstrated by our observations on mixtures of beads that form normal Watson–Crick pairs of complementary C_N/C'_N sticky ends (interaction scheme Ia, Fig. 1). Figure 2a shows the fraction of non-associated particles, or singlet fraction, as a function of time in an experiment where we first lowered the temperature from 52 to 20 °C ($t < 810$ s) and then ramped it back up ($t > 810$ s). Clearly, as soon as we go below the particles' dissociation temperature ($T_{dis} \approx 40$ °C), the singlet fraction quickly drops to zero, and the particles come together in extensive structures; conversely, when we increase the temperature above T_{dis} the aggregates quickly dissociate. The rate of temperature change determines how fast T_{dis} is reached, but it does not change the qualitative shape of the curves.

Much more flexibility is gained if the sticky ends possess secondary conformations, such as hairpins and loops due to intra-particle complementarity (for example, interaction scheme II, Fig. 1). Such secondary structures form in fractions of a microsecond, as estimated from the rotational diffusion time of single-stranded DNA with an end-to-end distance of ~14 nm. This should be compared with the association time of the particles, which depends on their diffusion constant and concentration, and which is of the order of minutes for micrometre-sized beads. As long as the secondary structures have smaller binding energies than the inter-particle bridges, particle association should in principle still be possible. However, in a fast temperature quench, extensive secondary structure formation will occur inside the DNA coatings of the individual beads before they encounter each other. Here, we explore the powerful *in situ* control that this novel self-protection mechanism offers over the number of sticky ends available for inter-particle bridging—one of the main parameters that determine the particles' association strength and kinetics[1,5,9,15–17]—and the new possibilities that this offers for the assembly of designer structures.

Figure 2b demonstrates that it is indeed the competition between the quench rate and the particles' diffusive encounter rate that matters. Unlike conventional DNA-functionalized particles (Fig. 2a), a fast temperature quench consistently arrests the aggregation of self-protective scheme II particles at a non-zero singlet fraction, which is higher for smaller particle concentrations (in Fig. 2b visible as a series of horizontal plateaux). The occurrence of aggregation followed by inactivation indicates that at the start of the quench, inter-particle bridges dominate, whereas at lower temperatures, intra-particle loop and hairpin formation reduce the number of unprotected sticky ends, to the point that it arrests the aggregation. At lower particle concentrations, fewer associative collisions occur before the interactions are completely inhibited, giving a higher plateau. The difference in the melting temperatures of the loops and inter-particle bridges, the former being lower than the latter, is due to the different configurational entropy costs[17] associated with these two hybridization geometries. Apparently, the particles' diffusive encounters, estimated to last ~0.2 ms, are too short for the low-temperature loops and hairpins to open up[18] and to form more stable inter-particle bridges. From Fig. 2b, it can also be seen that when the temperature is increased again ($t > 400$ s), dehybridization of the loops and hairpins reactivates the particle association, leading to a dip in the singlet fraction before the beads enter the familiar dissociation transition.

In addition to the quench rate/concentration dependence, Fig. 3 highlights two other important properties of our self-protected colloids. First, Fig. 3a shows the pronounced temperature dependence of the association kinetics in an experiment where we monitored the diffusive aggregation of scheme II beads at several different temperatures. From the inset, it is clear that the temperature response of these self-protective beads is much stronger than that of conventional scheme Ia beads. This results from the fact that the sticking probability of the self-protective beads depends on the fraction of unprotected sticky ends, which changes

[1]Center for Soft Matter Research, Physics Department, New York University, 4 Washington Place, New York 10003, USA, [2]Chemistry Department, New York University, 100 Washington Square East, New York 10003, USA. *e-mail: m.e.leunissen@nyu.edu.

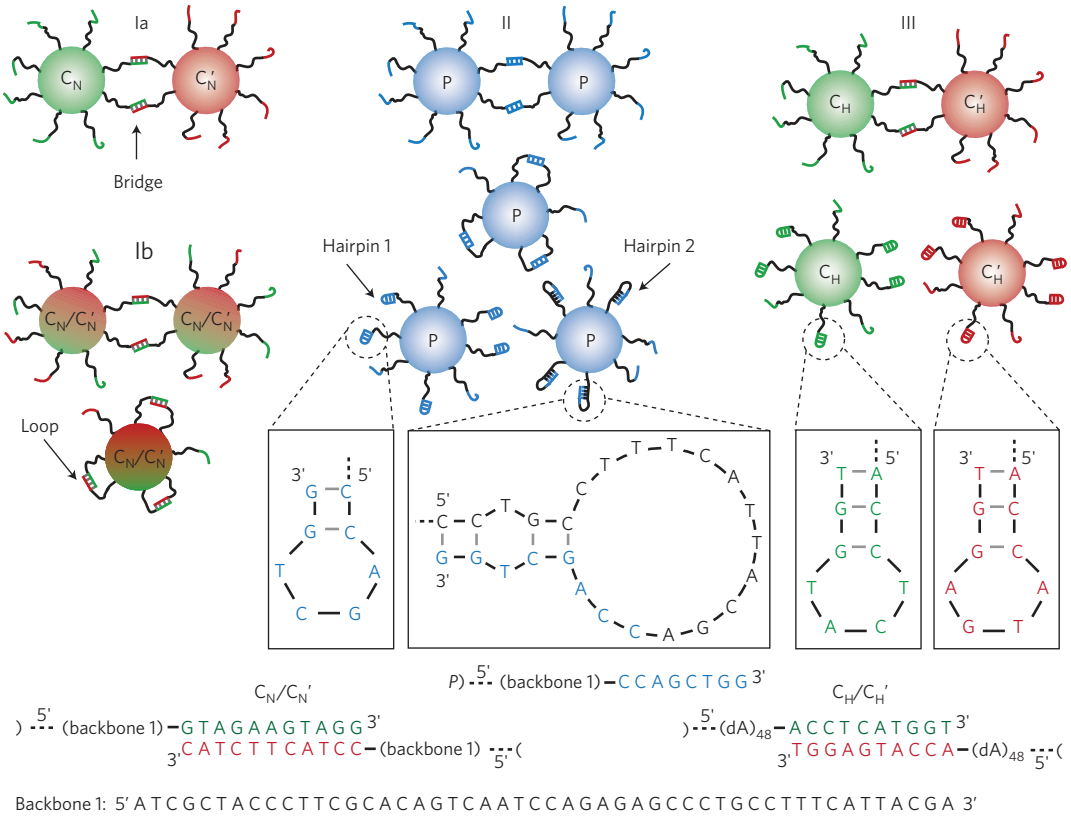

Figure 1 | Conventional and self-protected DNA-mediated interaction schemes. Schematic representation of the inter- and intra-particle DNA hybridization associated with the different experimental interaction schemes. Interaction scheme I involved a normal, secondary-structure free pair of complementary sticky ends, either grafted to separate beads (Ia) or mixed on the same bead (Ib). Interaction scheme II used a self-complementary, or palindromic, sticky end. Besides self-protective loops, this sequence can form two different hairpin structures: hairpin 1 involves only the sticky end sequence, whereas hairpin 2 forms between the sticky end and the backbone (for both $T_m \approx 34\,^{\circ}C$). Interaction scheme III consisted of a Watson–Crick pair on separate beads, where each of the sticky ends can form its own protective hairpin ($T_m \approx 43$–$45\,^{\circ}C$).

exponentially with the temperature, $f_U \propto \exp(\Delta G_{DNA}/k_B T)$ (here, ΔG_{DNA} represents the hybridization free energy of the protective secondary structures). For conventional beads, all sticky ends are always unprotected, making their association kinetics only weakly temperature dependent. Second, in Fig. 3b, we determined the fraction of scheme II particles that remained bound, after keeping them close together in chain-like structures, induced by a weak magnetic field[19]. The inset shows that the association kinetics again speed up with the temperature, but that the timescales are three orders of magnitude shorter than the ones associated with diffusive aggregation. This is because by keeping the particles in each other's proximity, the field allows for multiple binding attempts without slow, long-distance particle diffusion in between[19].

Taking advantage of the special properties of our self-protected colloids, we can overcome some of the main limitations of conventional DNA-functionalized systems. As an example, we demonstrate the directed assembly of ring-like structures, using interaction scheme II and holographic optical traps[20] (Fig. 4a–d). We either shrink a circular array of point-like traps until the particles are in close proximity (stationary trapping) or we use a continuous, rotating ring trap in which the particles can freely move around[21] (dynamic trapping). At high temperature, but well below the particles' dissociation transition, the self-protection is limited and the suspension behaves like a conventional DNA-functionalized system. This means that any positioning mistakes that occur while the particles are being arranged into the desired structure (the pre-assembly stage) immediately cause particles to stick in the wrong place. For instance, accidentally trapping two particles in the same stationary trap creates doublets (Fig. 4a and Supplementary Movie S1), whereas dynamic trapping yields only disordered clusters (Fig. 4a, inset and Supplementary Movie S2). In contrast, at low temperature the sticky ends are well protected, providing ample time to correct any positioning mistakes in the pre-assembly stage (Fig. 4b and Supplementary Movies S3a,b and S4a,b).

The particles inside the structures spontaneously bind together or can be triggered to do so by a brief elevation of the temperature. It follows from Fig. 3 that the temperature can be chosen such that the structures crosslink in ~5–10 min, whereas the diffusive aggregation is negligible for many hours. Thus, whereas at high temperatures the newly assembled structures soon aggregate and become decorated with other particles (Fig. 4c, e), at low temperatures the structures and surrounding suspension are nearly inert (Fig. 4d, f). These experiments also demonstrate that we can deliberately switch the association on and off without dissociating the previously assembled structures. Clearly, our self-protected particles greatly facilitate the fabrication of designer structures that are inert to further association, without the need to work under dilute conditions. Moreover, it enables multi-stage assembly approaches in which previously formed structures can for instance be isolated, transferred to a new particle suspension and kept stable for a prolonged time (Fig. 4h). These properties stand in sharp contrast to those of conventional DNA-functionalized systems that can switch only between fully associated and fully dissociated states[1,2,11,15,17] (note the finite-cluster phase in ref. 22, however). As is demonstrated by Fig. 4g, i, this limited control over conventional DNA-functionalized particles means that any newly assembled structure in these systems will be subject to rapid and uncontrollable aggregation, which compromises their practical use.

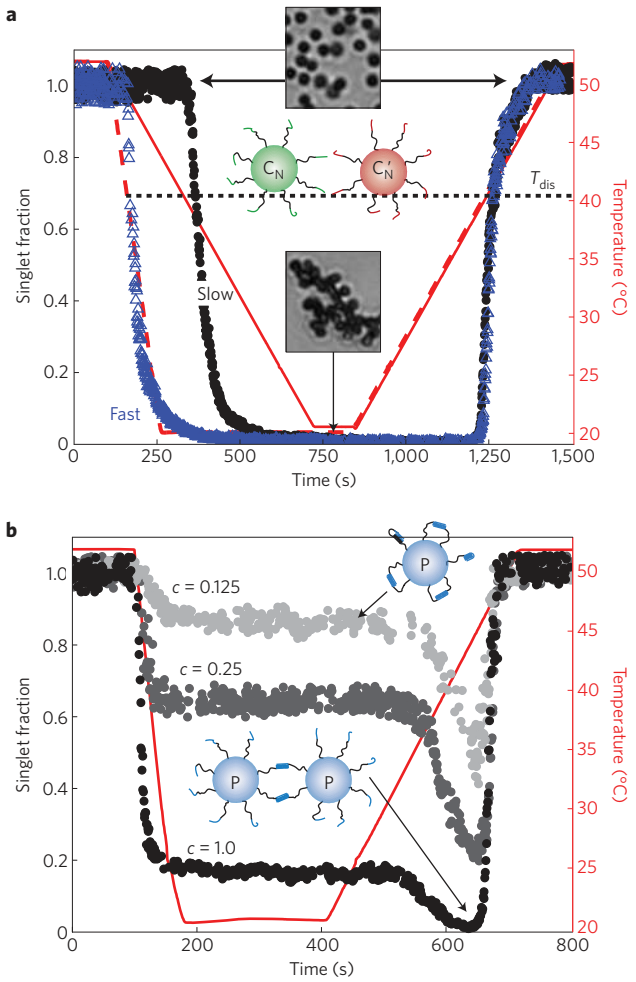

Figure 2 | Association–dissociation kinetics for conventional and self-protected interactions. a, Plot of the temperature (in red) and the corresponding particle singlet fraction (symbols) as a function of the elapsed time, for conventional interaction scheme Ia. The solid red line and black dots correspond to the slowest temperature quench; the dashed red line and blue triangles correspond to the fastest quench. The microscopy insets show a small part of the sample. **b**, Particle singlet fraction as a function of time for self-protected interaction scheme II and a fixed temperature profile, but at different overall particle concentrations ($c = 1.0$ corresponds to $\sim 2.8 \times 10^{11}$ particles per square metre).

A quantitative understanding of the self-protection can be obtained by modelling a series of association–dissociation curves that were obtained at different quench rates (Fig. 5a). Here, we outline the main principles; more details will be presented elsewhere. In its simplest form, we treat the particle association and dissociation as a reaction that interconverts singlets (S, concentration c_1) and doublets (S_2, concentration c_2):

$$2S \underset{k_{off}}{\overset{k_{on}}{\rightleftharpoons}} S_2$$

This reaction is governed by the rate equations:

$$\frac{dc_1}{dt} = -2k_{on}c_1^2 + 2k_{off}c_2$$
$$\frac{dc_2}{dt} = k_{on}c_1^2 - k_{off}c_2 \quad (1)$$

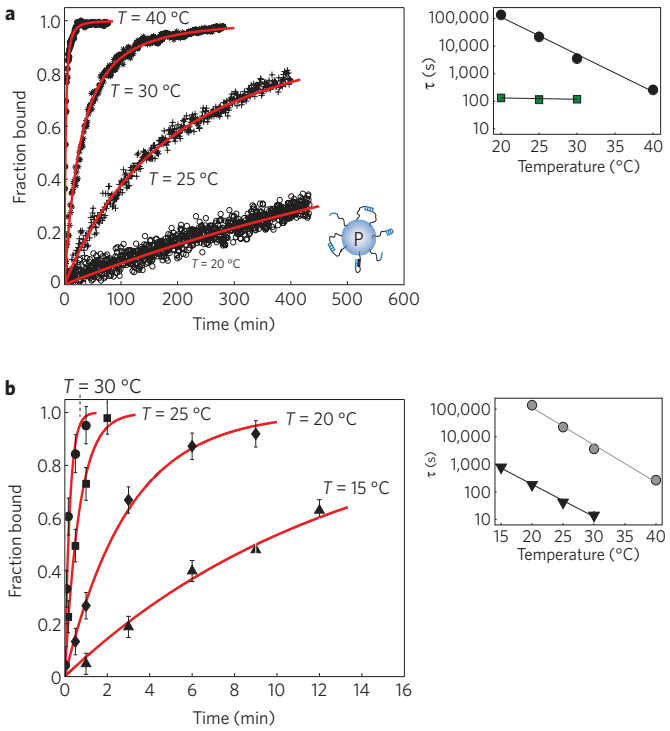

Figure 3 | Temperature response and proximity response of the switchable self-protected interactions. a, Fraction of aggregated scheme II particles as a function of time at different temperatures. The inset shows the characteristic aggregation times τ (black dots), obtained by fitting the data with the Smoluchowski aggregation equation, $f_{bound}(t) = 1-(1+t/\tau)^{-2}$. The τ values for conventional interaction scheme Ia are also shown (green squares). The error bars are approximately the size of the symbols. **b**, Plot of the fraction of scheme II particles that remained bound after keeping them close together in a weak magnetic field (~1 mT), for different field exposure times (horizontal axis) and temperatures. The inset shows the characteristic association time τ (black triangles), as obtained from first-order kinetics, $f_{bound}(t) = 1-\exp(-t/\tau)$. The diffusive aggregation times of the scheme II beads in **a** are reproduced in grey. All error bars result from the uncertainty in the singlet fraction obtained from image analysis.

In the experiments of Fig. 5a, each time t corresponds to a particular temperature, $T(t)$. The association rate parameter, k_{on}, depends on the diffusive flux of singlets, in two dimensions[23] $k_{diff} = 2k_B T(t)/3\eta R_p$ (k_B is the Boltzmann constant, η is the viscosity and R_p is the particle radius), and the dissociation rate parameter follows from the free energy for bead–bead hybridization, $k_{off}(t) \propto \exp(\Delta F_{bead}/k_B T)$. The horizontal plateaux in the experimental aggregation curves indicate that the conversion of loops and hairpins into inter-particle bridges occurs on a timescale that is significantly longer than the duration of a diffusive particle encounter. Moreover, by the time two particles encounter each other, a hybridization equilibrium will have been established inside their DNA coatings. Therefore, we assume that in the early stages of association, ΔF_{bead} is determined by the fraction of unprotected sticky ends at the moment of collision, which follows from the partition function of all of the different hybridization possibilities[24] on an isolated particle, Supplementary Equations S1–S3 and schematic diagram 1, Fig. 5b. Using the predicted solution hybridization free energies, ΔG^0 (see the Methods section), and including an appropriate configurational entropy cost, ΔS_{conf}, for the loops ($\Delta G_{loop} = \Delta G^0_{p,solution} - T\Delta S_{conf,loop}$) (ref. 17), we find the bond distributions in Fig. 5c. Taking the fraction of unprotected sticky ends, f_{AU}, we obtain ΔF_{bead} from the expression that we

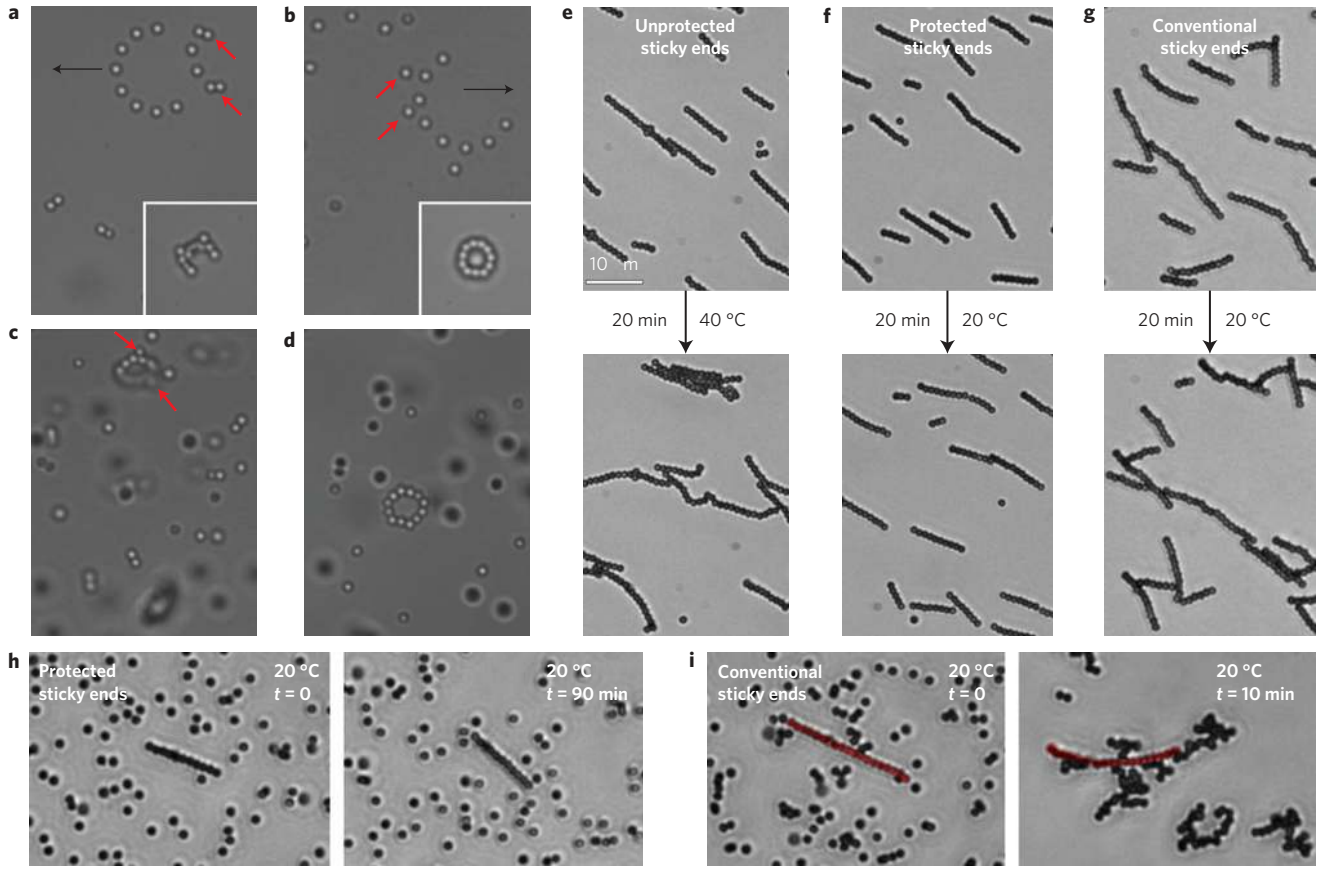

Figure 4 | Directed assembly using self-protected interactions as a 'nano-contact glue'. a, Microscopy image of scheme II particles in a circular array of optical traps, at high temperature ($T \approx 27\,^{\circ}C$). The black arrow indicates a displacement of the array, causing the release of two accidentally formed doublets (red arrows). Inset: Example of the disordered clusters that were obtained at high temperature in a rotating ring trap. **b**, As in **a**, but at low temperature ($T \approx 20\,^{\circ}C$). Displacement of the array releases superfluous particles from doubly occupied traps (red arrows), without forming unwanted doublets. Inset: A properly formed ring structure from a rotating ring trap at low temperature. **c**, After 20 min at 27 °C, multiple suspension particles stuck to the previously assembled ring structure (red arrows). **d**, This does not happen at low temperature (20 °C). **e**,**f**, Linear chains of scheme II particles, made with magnetic traps, were kept for 20 min at $T = 40\,^{\circ}C$ (**e**) and $T = 20\,^{\circ}C$ (**f**). **g**, The results of a similar experiment with conventional sticky ends, which cannot form protective secondary structures. **h**, A linear chain of scheme II particles was isolated and transferred to a new suspension of the same particles, after which it was kept inert for a prolonged time at low temperature (20 °C). **i**, The results of a similar transfer experiment with conventional DNA-functionalized particles; the original chain is shown in red. In all images, the particles were ~1.0 μm in diameter.

derived in ref. 17 for two surfaces that interact with a certain fixed number of active sticky ends:

$$\frac{\Delta F_{\mathrm{bead}}}{k_{\mathrm{B}}T} = -\ln\left(\left[1 + f_{\mathrm{AU}} m \exp\left(-\frac{\Delta G_{\mathrm{bridge}}}{k_{\mathrm{B}}T}\right)\right]^{f_{\mathrm{AU}}N_b} - 1\right)$$

Here, N_{b} is the maximum number of bridges that can form if all sticky ends are unprotected, m is the number of opposing sticky ends within reach and $\Delta G_{\mathrm{bridge}} = \Delta G^{0}_{\mathrm{P,solution}} - T\Delta S_{\mathrm{conf,bridge}}$.

To model the particles' high-temperature dissociation transition ($t \gg 810$ s in Fig. 5a) we follow a similar approach, but now we consider the equilibrium that includes intra- and inter-particle hybridization simultaneously, because the particles inside the aggregates are in prolonged contact, enabling the interconversion of loops, hairpins and inter-particle bridges. The total partition function and ΔF_{bead} are then given by Supplementary Equations S4–S8 (see also schematic diagram 2, Fig. 5b), and Fig. 5d shows the bond distributions. Finally, we fit the experimental data by numerically solving for the evolution of the rate equations (equation (1)), using the experimental singlet concentration at $t = 0$ and temperature profiles, $T(t)$, as input. Keeping all other parameters fixed at their known or estimated values, we obtained the fits in Fig. 5a with the configurational entropy costs $\Delta S_{\mathrm{conf,bridge}} = -12.6k_{\mathrm{B}}$ and $\Delta S_{\mathrm{conf,loop}} = -13.5 \pm 0.2k_{\mathrm{B}}$. In ref. 17, we have shown that these values agree fairly well with those obtained from simple geometrical estimates. Moreover, the computed curves show the expected strong dependence on the quench rate.

Figure 5c indicates that for interaction scheme II, the main contribution to the self-protection comes from loop formation. We verified this with a system in which the normal C_{N} and C'_{N} sticky ends were mixed in a 50/50 ratio on the same bead, giving loop formation, but no hairpins (interaction scheme Ib, Fig. 1). Figure 5e shows that in broad lines the association–dissociation behaviour for this system is indeed similar to that of scheme II. However, the $C_{\mathrm{N}}/C'_{\mathrm{N}}$ system suffers from a 'pairing' problem, in that a certain fraction of sticky ends fails to find a nearby partner for loop formation. This prevents a complete arrest of the aggregation, hence the tilt of the plateaux in Fig. 5e. Apparently, the seemingly insignificant hairpin formation of scheme II has an important role in circumventing the pairing problem, as the mono-molecular hairpins protect sticky ends that remain without a binding partner. We also point out that similar switchable self-protected interactions can be established with sticky ends that form only hairpins and that have no intra-particle complementarity, such as, for instance, the $C_{\mathrm{H}}/C'_{\mathrm{H}}$ pair of interaction scheme III (Fig. 1 and Supplementary Fig. S1).

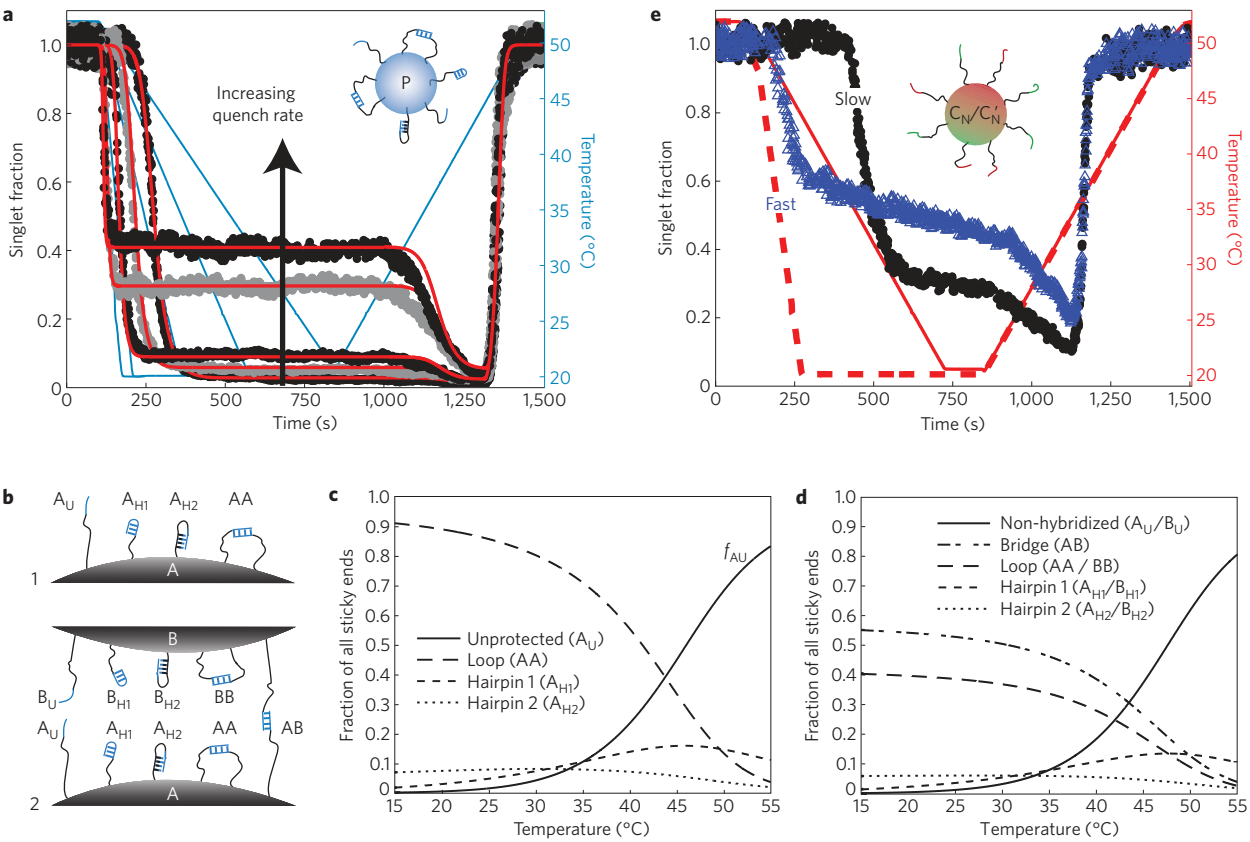

Figure 5 | Experimental and modelled association–dissociation kinetics. a, Experimentally recorded particle singlet fraction (dots) as a function of time for self-protected interaction scheme II and different temperature ramps (in blue). The red lines show the fits from our theoretical model. **b**, Our nomenclature for the different hybridization possibilities on an isolated scheme II bead (1) and for two such beads in contact (2). **c**, Calculated bond distributions on an isolated scheme II bead, as a function of temperature. **d**, As in **c**, but for two beads in contact. **e**, Plot of the temperature (in red) and the corresponding particle singlet fraction (symbols) as a function of the elapsed time, for interaction scheme Ib. The solid red line and black dots correspond to the slowest temperature quench; the dashed red line and blue triangles correspond to the fastest quench.

We have added secondary structure formation to the DNA toolkit that facilitates the (self-)assembly of nanometre- and micrometre-sized particles[25], and we have developed a model that provides a quantitative understanding of the particle association. Besides facilitating the fabrication of designer structures, the self-protected interactions will impart selective, self-healing and self-reinforcing properties to the particle assemblies. Selective, because particles only connect if held sufficiently long in the right position; here done with optical or magnetic traps, but other methods, such as templating, are conceivable as well. Self-healing, because the material can be broken into smaller, stable pieces that nevertheless have the ability to reconnect[26]. Self-reinforcing, because the initially weak bridging may be followed by the formation of more bonds through the opening of intra-particle loops and hairpins, either spontaneously or triggered by heat. The last property is reminiscent of certain forms of cell adhesion, where rapid capture is followed by slow consolidation[27], and, together with the other functionalities, this will enable more complex assembly schemes.

Methods

DNA and particle preparation. All of our DNA constructs consisted of a highly flexible, single-stranded backbone of 50 nucleotides long with a short, 8–11 nucleotides long single-stranded sequence at its 3′ terminus. We purchased the C_N/C'_N and P oligonucleotides from Integrated DNA Technologies USA, whereas we synthesized the C_H/C'_H sequences ourselves, on an Applied Biosystems 394 DNA synthesizer. After completion, we removed the oligonucleotides from the support and deprotected them using routine phosphoramidite procedures[28]. The backbone of the DNA constructs was attached to a 5′ biotin group through a short, flexible polyethyleneglycol spacer. For most experiments, we functionalized 1.05-μm-diameter, streptavidin-coated, paramagnetic polystyrene Dynabeads (MyOne Streptavidin C1, Molecular Probes) with the biotinylated DNA constructs, by incubating 5 μl bead suspension for 30 min at 55 °C with 5 μl of 6 μM oligonucleotide solution and 65 μl suspension buffer (10 mM phosphate/50 mM NaCl and 0.5% w/w Pluronic surfactant F127, pH 7.5). Strong sedimentation of these high-density particles quickly led to essentially two-dimensional microscopy samples. For the optical trapping experiments, we used 1.0-μm-diameter, non-fluorescent, neutravidin-labelled polystyrene Fluospheres (Invitrogen), combining 5 μl bead suspension with 10 μl oligonucleotide solution and 85 μl suspension buffer. These particles had a density close to that of water and remained suspended throughout the entire sample for many hours. In all cases, we removed excess and non-specifically adsorbed DNA by centrifuging and resuspending the particles three times in 100 μl suspension buffer; we repeated this washing procedure twice, heating in between for 30 min at 55 °C.

Thermodynamic parameters of the oligonucleotides. We obtained the enthalpic and entropic contributions to the hybridization free energies ($\Delta G^0 = \Delta H^0 - T\Delta S^0$) of the sticky ends and their secondary structures from the Mfold webserver[29,30], using $[Na^+] = 68$ mM for the suspension buffer. C_N/C'_N: $\Delta H^0 = -370$ kJ mol^{-1}, $\Delta S^0 = -1.08$ kJ mol^{-1} K^{-1}; P: $\Delta H^0 = -296$ kJ mol^{-1}, $\Delta S^0 = -841$ J mol^{-1} K^{-1}; P hairpin 1: $\Delta H^0 = -84.9$ kJ mol^{-1}, $\Delta S^0 = -276$ J mol^{-1} K^{-1}; P hairpin 2: $\Delta H^0 = -148$ kJ mol^{-1}, $\Delta S^0 = -472$ J mol^{-1} K^{-1}; C_H/C'_H: $\Delta H^0 = -285$ kJ mol^{-1}, $\Delta S^0 = -798$ J mol^{-1} K^{-1}; C_H hairpin: $\Delta H^0 = -81.6$ kJ mol^{-1}, $\Delta S^0 = -258$ J mol^{-1} K^{-1}; C'_H hairpin: $\Delta H^0 = -71.1$ kJ mol^{-1}, $\Delta S^0 = -223$ J mol^{-1} K^{-1}.

Light microscopy set-up. For the various association studies, we confined the DNA-functionalized particle suspensions to a borosilicate glass capillary (inner dimensions 2.0 × 0.1 mm, Vitrocom), which was previously cleaned by oxygen plasma etching and hydrophobized by silanization. The capillary was then mounted on a special stage set-up on a Leica DMRXA light microscope, which enabled fine temperature control, while imaging in transmission mode (see the description in ref. 31). To study the association kinetics in the presence of a magnetic field, we centred the iron cores of an electromagnet coil (made in-house) around the microscope objective.

Temperature-regulated holographic optical trapping set-up. For optical trapping, 10 µl of DNA-functionalized particle suspension was sealed between two $18 \times 18\ mm^2$, number 1 cover slips, which were previously cleaned by oxygen plasma etching and hydrophobized by silanization. The sample then was mounted on a sapphire microscope slide and centred on a 14.5-mm-diameter hole passing through a water-cooled Peltier element (Melcor, series SH 1.0-95-06). This enabled us to control the sample's temperature while simultaneously providing optical access for transmission-mode imaging and optical micromanipulation. Holographic optical traps were powered by a frequency-doubled diode-pumped solid-state laser (Coherent Verdi), operating at a wavelength of 532 nm. A reflective liquid crystal spatial light modulator (Hamamatsu X8267-16 PPM) imprinted the beam's wavefronts with computer-generated holograms encoded with the desired trapping pattern. This laser profile was then directed into the input pupil of a ×100, numerical aperture: 1.4, Plan Apo oil-immersion objective mounted on a Nikon TE-2000U inverted optical microscope, and was focused into optical traps.

Received 26 February 2009; accepted 15 May 2009; published online 14 June 2009

References

1. Maye, M. M., Nykypanchuk, D., van der Lelie, D. & Gang, O. DNA-regulated micro- and nanoparticle assembly. *Small* **3**, 1678–1682 (2007).
2. Mirkin, C. A., Letsinger, R. L., Mucic, R. C. & Storhoff, J. J. A DNA-based method for rationally assembling nanoparticles into macroscopic materials. *Nature* **382**, 607–609 (1996).
3. Tkachenko, A. V. Morphological diversity of DNA-colloidal self-assembly. *Phys. Rev. Lett.* **89**, 148303 (2002).
4. Licata, N. A. & Tkachenko, A. V. Errorproof programmable self-assembly of DNA-nanoparticle clusters. *Phys. Rev. E* **74**, 041406 (2006).
5. Biancaniello, P. L., Kim, A. J. & Crocker, J. C. Colloidal interactions and self-assembly using DNA hybridization. *Phys. Rev. Lett.* **94**, 058302 (2005).
6. Nykypanchuk, D., Maye, M. M., van der Lelie, D. & Gang, O. DNA-guided crystallization of colloidal nanoparticles. *Nature* **451**, 549–552 (2008).
7. Park, S. Y. *et al.* DNA-programmable nanoparticle crystallization. *Nature* **451**, 553–556 (2008).
8. Kim, A. J., Scarlett, R., Biancaniello, P. L., Sinno, T. & Crocker, J. C. Probing interfacial equilibration in microsphere crystals formed by DNA-directed assembly. *Nature Mater.* **8**, 52–55 (2009).
9. Xiong, H., van der Lelie, D. & Gang, O. Phase behavior of nanoparticles assembled by DNA linkers. *Phys. Rev. Lett.* **102**, 015504 (2009).
10. Milam, V. T., Hiddessen, A. L., Crocker, J. C., Graves, D. J. & Hammer, D. A. DNA-driven assembly of bidisperse, micron-sized colloids. *Langmuir* **19**, 10317–10323 (2003).
11. Valignat, M. P., Theodoly, O., Crocker, J. C., Russel, W. B. & Chaikin, P. M. Reversible self-assembly and directed assembly of DNA-linked micrometer-sized colloids. *Proc. Natl Acad. Sci. USA* **102**, 4225–4229 (2005).
12. Yurke, B., Turberfield, A. J., Mills, A. P. J., Simmel, F. C. & Neumann, J. L. A DNA-fuelled molecular machine made of DNA. *Nature* **406**, 605–608 (2000).
13. Yan, H., Zhang, X., Shen, Z. & Seeman, N. C. A robust DNA mechanical device controlled by hybridization topology. *Nature* **415**, 62–65 (2002).
14. Aldaye, F. A., Palmer, A. L. & Sleiman, H. F. Assembling materials with DNA as the guide. *Science* **321**, 1795–1799 (2008).
15. Jin, R., Wu, G., Li, Z., Mirkin, C. A. & Schatz, G. C. What controls the melting properties of DNA-linked gold nanoparticle assemblies? *J. Am. Chem. Soc.* **125**, 1643–1654 (2003).
16. Nykypanchuk, D., Maye, M. M., van der Lelie, D. & Gang, O. DNA-based approach for interparticle interaction control. *Langmuir* **23**, 6305–6314 (2007).
17. Dreyfus, R. *et al.* Simple quantitative model for the reversible association of DNA coated colloids. *Phys. Rev. Lett.* **102**, 048301 (2009).
18. Bonnet, G., Krichevsky, O. & Libchaber, A. Kinetics of conformational fluctuations in DNA hairpin-loops. *Proc. Natl Acad. Sci. USA* **95**, 8602–8606 (1998).
19. Baudry, J. *et al.* Acceleration of the recognition rate between grafted ligands and receptors with magnetic forces. *Proc. Natl Acad. Sci. USA* **103**, 16076–16078 (2006).
20. Grier, D. G. A revolution in optical manipulation. *Nature* **424**, 810–816 (2003).
21. Roichman, Y., Sun, B., Roichman, Y., Amato-Grill, J. & Grier, D. G. Optical forces arising from phase gradients. *Phys. Rev. Lett.* **100**, 013602 (2008).
22. Schmatko, T. *et al.* A finite-cluster phase in λ-DNA-coated colloids. *Soft Matter* **3**, 703–706 (2007).
23. Smoluchowski, M. V. Versuch einer mathematischen theorie der koagulationskinetik kolloider lösungen. *Z. Phys. Chem.* **92**, 129–168 (1917).
24. Dimitrov, R. A. & Zuker, M. Prediction of hybridization and melting for double-stranded nucleic acids. *Biophys. J.* **87**, 215–226 (2004).
25. Crocker, J. C. Nanomaterials: Golden handshake. *Nature* **451**, 528–529 (2008).
26. Cordier, P., Tournilhac, F., Soulie-Ziakovic, C. & Leibler, L. Self-healing and thermoreversible rubber from supramolecular assembly. *Nature* **451**, 977–980 (2008).
27. von Andrian, U. H. *et al.* Two-step model of leukocyte endothelial cell interaction in inflammation: Distinct roles for LECAM-1 and the leukocyte β2 integrins *in vivo*. *Proc. Natl Acad. Sci. USA* **88**, 7538–7542 (1991).
28. Caruthers, M. H. Gene synthesis machines: DNA chemistry and its uses. *Science* **230**, 281–285 (1985).
29. Zuker, M. Mfold web server for nucleic acid folding and hybridization prediction. *Nucleic Acids Res.* **31**, 3406–3415 (2003).
30. Zuker, M. <http://mfold.bioinfo.rpi.edu/>.
31. Leunissen, M. E. *et al.* Towards self-replicating materials of DNA-functionalized colloids. *Soft Matter* doi:10.1039/B817679E (2009).

Acknowledgements

We thank D. J. Pine and M. Zuker for useful discussions. This work was supported partially by the MRSEC Program of the National Science Foundation under Award Number DMR-0820341, by the Keck Foundation and the Netherlands Organisation for Scientific Research (NWO) .

Author contributions

M.E.L. carried out the experiments, theoretically modelled the data and wrote the manuscript. R.D. was involved in setting up the experiments and the development of the model, F.C.C. and D.G.G. participated in the optical laser tweezer experiments, R.S. and N.C.S. synthesized DNA and P.M.C. supervised the research. Everybody contributed important conceptual insight.

Additional information

Supplementary information accompanies this paper on www.nature.com/naturematerials. Reprints and permissions information is available online at http://npg.nature.com/reprintsandpermissions. Correspondence and requests for materials should be addressed to M.E.L.